

A critical role for histone H2AX in recruitment of repair factors to nuclear foci after DNA damage

Tanya T. Paull*, Emmy P. Rogakou[†], Vikky Yamazaki[‡], Cordula U. Kirchgessner[‡], Martin Gellert* and William M. Bonner[†]

Background: The response of eukaryotic cells to double-strand breaks in genomic DNA includes the sequestration of many factors into nuclear foci. Recently it has been reported that a member of the histone H2A family, H2AX, becomes extensively phosphorylated within 1–3 minutes of DNA damage and forms foci at break sites.

Results: In this work, we examine the role of H2AX phosphorylation in focus formation by several repair-related complexes, and investigate what factors may be involved in initiating this response. Using two different methods to create DNA double-strand breaks in human cells, we found that the repair factors Rad50 and Rad51 each colocalized with phosphorylated H2AX (γ -H2AX) foci after DNA damage. The product of the tumor suppressor gene BRCA1 also colocalized with γ -H2AX and was recruited to these sites before Rad50 or Rad51. Exposure of cells to the fungal inhibitor wortmannin eliminated focus formation by all repair factors examined, suggesting a role for the phosphoinositide (PI)-3 family of protein kinases in mediating this response. Wortmannin treatment was effective only when it was added early enough to prevent γ -H2AX formation, indicating that γ -H2AX is necessary for the recruitment of other factors to the sites of DNA damage. DNA repair-deficient cells exhibit a substantially reduced ability to increase the phosphorylation of H2AX in response to ionizing radiation, consistent with a role for γ -H2AX in DNA repair.

Conclusions: The pattern of γ -H2AX foci that is established within a few minutes of DNA damage accounts for the patterns of Rad50, Rad51, and Brca1 foci seen much later during recovery from damage. The evidence presented strongly supports a role for the γ -H2AX and the PI-3 protein kinase family in focus formation at sites of double-strand breaks and suggests the possibility of a change in chromatin structure accompanying double-strand break repair.

Background

The introduction of double-strand breaks into DNA triggers a complex set of responses in eukaryotic cells, including cell cycle arrest, relocalization of DNA repair factors, and in some cases apoptosis. Failure to arrest cellular functions can lead to a high level of genomic instability, which is linked to increased probabilities of oncogenic transformation. Several factors known to be involved in DNA repair or in signalling the presence of damage have been shown to accumulate in large nuclear domains (foci) after double-strand DNA breakage [1–6]. This response is not yet fully understood but has been suggested to be a visual indication of DNA repair centers.

The Mre11–Rad50–Nbs1 (MRN) complex, for instance, has been shown to form foci after exposure to ionizing radiation [1] and these foci localize to subnuclear volumes containing the damaged DNA [7]. The analogous complex

in *Saccharomyces cerevisiae* (Mre11–Rad50–Xrs2) functions in the cellular response to ionizing radiation [8–10] as well as in non-homologous end-joining [11,12], meiotic recombination [9,10,13], and telomere maintenance [14–16], and may also play a role in homologous recombination [17,18]. The MRN complex exhibits exo- and endonuclease activities, consistent with a role for DNA end processing during repair of double-strand breaks [19–21].

The eukaryotic RecA homolog Rad51 forms foci at sites of single-stranded DNA following DNA damage and, unlike MRN, forms foci in untreated cells during S phase [22]. Interestingly, Rad50 foci and Rad51 foci are rarely found in the same cell after damage [1,23], suggesting that there might be two mutually exclusive pathways of repair. The product of the Brca1 tumor suppressor gene also colocalizes separately with Rad50 or Rad51, fueling speculation of a role for Brca1 in DNA double-strand break repair [4,23].

Addresses: *Laboratory of Molecular Biology, National Institute of Diabetes and Digestive and Kidney Diseases, National Institutes of Health, Bethesda, Maryland 20892-0540, USA. [†]Laboratory of Molecular Pharmacology, Division of Basic Sciences, National Cancer Institute, National Institutes of Health, Bethesda, Maryland 20892, USA. [‡]Department of Radiation Oncology, Mayer Cancer Research Laboratory, School of Medicine, Stanford University, Stanford, California 94305, USA.

Correspondence: Martin Gellert
E-mail: gellert@helix.nih.gov

Received: 17 April 2000
Revised: 25 May 2000
Accepted: 19 June 2000

Published: 11 July 2000

Current Biology 2000, 10:886–895

0960-9822/00/\$ – see front matter
© 2000 Elsevier Science Ltd. All rights reserved.

One of the first cellular responses to the introduction of double-strand breaks is the phosphorylation of H2AX, one of three types of histone H2A molecules in eukaryotic cells [24]. Serine 139 in the unique carboxy-terminal tail of H2AX is phosphorylated within 1 to 3 minutes after damage, and the number of H2AX molecules phosphorylated increases linearly with the severity of the damage. Introduction of double-strand breaks elicits this response, but other types of damage, for instance UV irradiation, do not. An antibody specific to the phosphorylated form of H2AX (γ -H2AX) was produced recently and used to show that γ -H2AX is localized in large chromatin domains at the sites of DNA damage [25].

Given the very rapid and specific modification of H2AX after formation of double-strand breaks, we asked whether the foci of these phosphorylated molecules might be related to the foci of repair factors usually observed at much later time points after DNA damage. In this work, using both a laser scissors apparatus and a ^{137}Cs source of ionizing radiation to induce double-strand breaks, we found that the initial pattern of γ -H2AX molecules formed in the nucleus corresponds to the pattern of both Rad50 and Rad51 types of damage-induced foci, which appear later in the recovery. Brca1 is also recruited to these structures, and appears much earlier than the other repair factors investigated. Interference with H2AX phosphorylation by the kinase inhibitor wortmannin, or the use of a kinase-defective cell line, provides further evidence for the role of phosphorylated H2AX in initiating focus formation by repair factors after DNA damage, and for the involvement of phosphoinositide (PI)-3 kinases in activating H2AX.

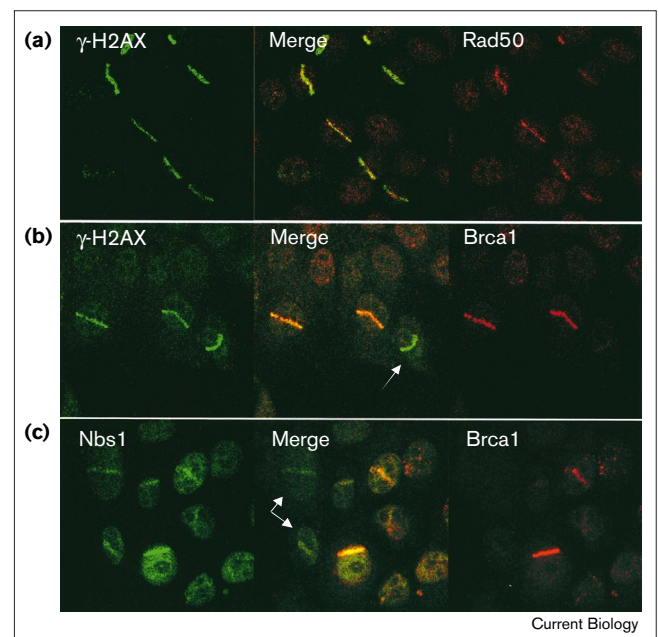
Results

Colocalization of γ -H2AX and repair factors at sites of laser-induced double-strand breaks

To determine whether any of the known repair-related factors colocalizes with γ -H2AX after DNA damage, we used a technique in which cells grown in the presence of a low concentration of BrdU are then incubated with a DNA intercalating dye (Hoechst 33258) and exposed to UV light, which causes double-strand breaks to occur in genomic DNA at sites of BrdU incorporation [26]. Instead of a general UV light source, we used a 390 nm dye laser in a 'laser scissors' apparatus to introduce the breaks into living cells, as described recently [25]. In this procedure, the cells (grown on a coverslip) are mounted on the microscope stage, which is then moved relative to the laser beam.

Human cells from the breast tumor line MCF7 were irradiated using the laser scissors technique and allowed to recover for 30 minutes before fixation and antibody staining. As shown in Figure 1a, immunostaining with antibodies directed against γ -H2AX (green) and Rad50 (red) revealed that both molecules localized specifically in the

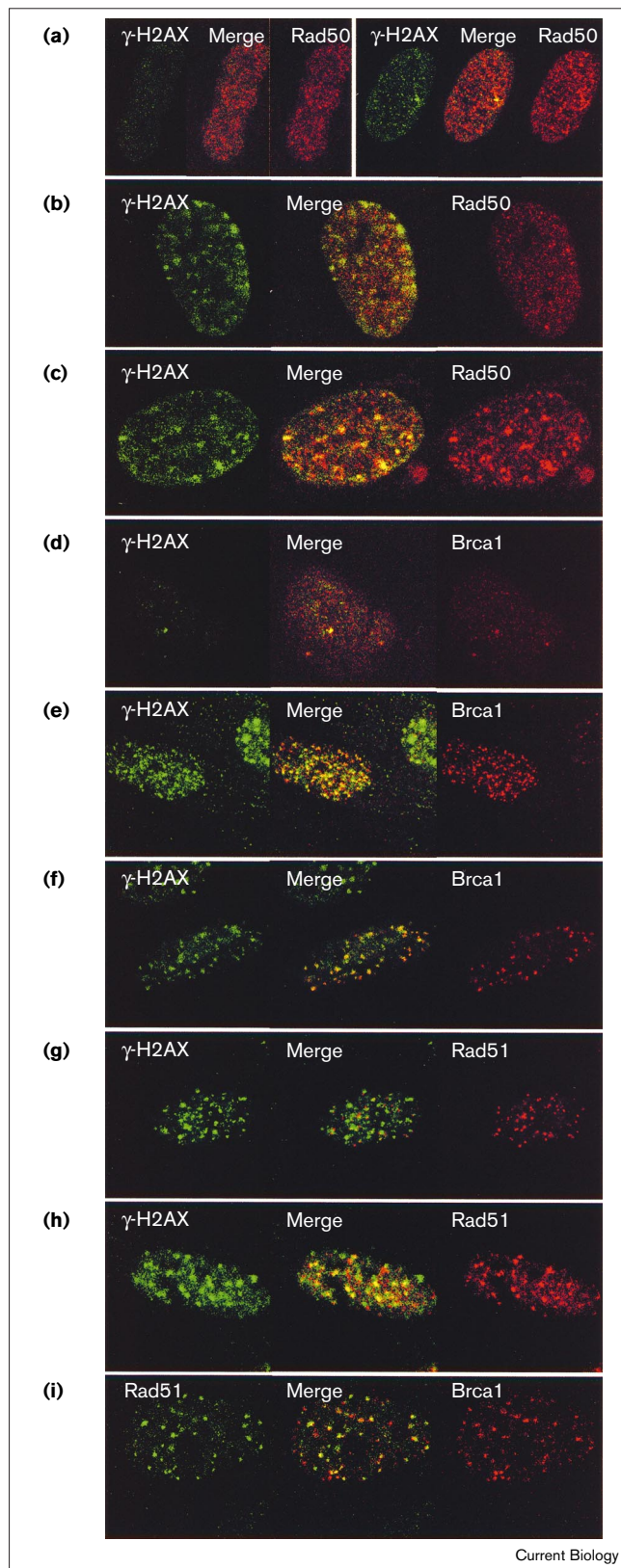
Figure 1



Rad50, Nbs1, and Brca1 localize to γ -H2AX and sites of double-strand breaks introduced by laser scissors. **(a)** MCF7 cells, irradiated at 30% power, recovered for 30 min at 37° before fixation, permeabilization, and staining with primary antibodies directed against γ -H2AX (green) and Rad50 (red) as indicated. **(b)** MCF7 cells were irradiated at 10% power with a recovery of 30 min before fixation. An antibody directed against Brca1 (red) was used in addition to the γ -H2AX antibody (green), as indicated. The arrow in the merged image indicates a cell which has very strong γ -H2AX staining but weak Brca1 staining. **(c)** Cells were treated as in (b) except with antibodies directed against Brca1 (red) and Nbs1 (green). The arrows in the merged image indicate cells which have Nbs1 staining but do not have Brca1 foci.

pattern of the laser path through the cell nuclei. Thus, the MRN complex clearly localizes to sites of H2AX phosphorylation at the locations of double-strand breaks.

Immunofluorescence studies of Brca1 have shown colocalization with Rad51 in bright foci after DNA damage [4]. To investigate the relationship between Brca1 and γ -H2AX phosphorylation, we introduced double-strand breaks with the laser scissors and stained with antibodies specific for each protein. As shown in Figure 1b, Brca1 localized exactly to the line of DNA breaks and to γ -H2AX. Formation of this line pattern was evident with Brca1 antibody staining in most, but not all, of the cells with a γ -H2AX pattern. Because Brca1 has been reported to colocalize with the MRN complex [23], we also tried a combination of Brca1 and Nbs1 antibodies and found that the two factors often colocalized together to the lines of DNA breakage (Figure 1c). Several cells, however, exhibited a Nbs1 staining pattern but not a Brca1 staining pattern. Our results with the laser scissors suggest that the MRN complex and Brca1 do localize to γ -H2AX and

**Figure 2**

Colocalization of Rad50, Brca1, and Rad51 with γ -H2AX foci. (a–c) IMR90 cultures were untreated (a) or irradiated with 12 Gy and allowed to recover at 37° for (b) 2 h or (c) 6 h before fixation and antibody staining. Samples were incubated with antibodies directed against γ -H2AX (green) and Rad50 (red). The cell shown on the left in (a) is representative of the majority of the cells in the population. The cell shown on the right in (a) is representative of the 5–10% of the unirradiated cells which exhibit γ -H2AX foci. (d–f) IMR90 cells were (d) untreated or (e,f) irradiated with 12 Gy and allowed to recover for (e) 2 h or (f) 6 h before fixation and staining with antibodies directed against γ -H2AX (green) and Brca1 (red). (g,h) Irradiated cultures recovered for (g) 2 h or (h) 6 h and were incubated with antibodies directed against γ -H2AX (green) and Rad51 (red). (i) Irradiated cells recovered for 6 h and were stained with antibodies directed against Rad51 (green) and Brca1 (red). The cells shown in (d–i) are representative of the 10–20% of the total population that contain Brca1 foci.

Sequential assembly of repair factors after ionizing radiation

To examine the effects of lower doses of radiation and to extend our study to cell lines less tolerant of the laser scissors procedure, we used a standard ^{137}Cs source to introduce double-strand breaks. The time course of focus formation in the normal fibroblast line IMR90 after 12 Gy irradiation was examined in comparison to unirradiated cells, using pairwise combinations of antibodies specific to γ -H2AX, Rad50 (or Nbs1), Brca1, and Rad51, as shown in Figure 2. In unirradiated IMR90 cells, we observed two distinct populations with respect to γ -H2AX. In 90–95% of the cells, the γ -H2AX staining was extremely weak and diffuse (Figure 2a, left), whereas in 5–10% of the cells, we observed one or a few bright γ -H2AX foci (Figure 2a, right). Within this smaller population of cells, the few γ -H2AX foci colocalized with Rad50 foci in a majority of the cells we examined, suggesting that the MRN complex is recruited to double-strand breaks that occur in the absence of irradiation.

After exposure of IMR90 cells to 12 Gy ionizing radiation, γ -H2AX foci appeared in 100% of the cell population (data not shown). In contrast, Rad50 foci appeared more slowly, over a period of several hours (Figure 2b,c), as described previously for this cell line [1]. At the 2 hour time point, for instance, γ -H2AX foci were clearly present in the absence of Rad50 foci (Figure 2b). However, when the Rad50 foci did appear at 6–8 hours post-irradiation, they coincided significantly with the γ -H2AX foci already present (Figure 2c). Colocalization of Rad50 with γ -H2AX continued through at least 24 hours, although the number of foci in each cell decreased at the later times (data not shown). A quantitative assessment of this colocalization was made using the software program NIH Image to count all of the foci in at least 30 cells per time point (Figure 3a). These data indicated that the number of γ -H2AX–Rad50 colocalizing foci increased gradually and reached a maximum by 6–8 hours after irradiation, at

to sites of DNA double-strand breaks but that the association of Brca1 with MRN is seen only in a subset of the cell population.

which time approximately 70% of γ -H2AX foci coincided with Rad50 foci.

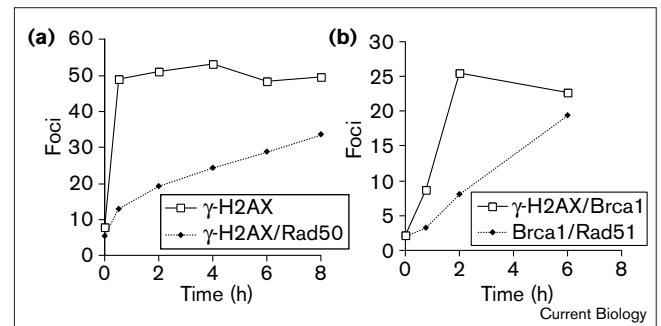
Brca1 recruitment into foci after DNA damage

We then examined the time course of Brca1 focus formation in IMR90 cells (Figure 2d–f) and found that it differed significantly from the time course of Rad50 colocalization. Before irradiation, 10–15% of the cell population exhibited Brca1 foci and approximately 50–70% of these cells had at least one Brca1 focus colocalizing with a γ -H2AX focus (as in Figure 2d). After 12 Gy irradiation and 45 minutes recovery, the S-phase Brca1 foci disappeared (data not shown), consistent with previous reports [4]. After 2 hours of recovery, the IMR90 cells exhibited Brca1 foci in 10–15% of the population and in these cells the majority of the Brca1 foci overlapped γ -H2AX foci (Figure 2e). Both visual analysis and quantification of foci (Figure 3b) showed that the density of Brca1/ γ -H2AX colocalized foci reached a maximum by 2 hours after irradiation, thus considerably earlier than the Rad50/ γ -H2AX foci. The Brca1 foci were not at their maximum brightness at this time, but the subnuclear locations of at least 60% of Brca1 foci in each cell coincided with γ -H2AX foci by 2 hours of recovery after irradiation. Colocalization of Brca1 with γ -H2AX continued through the 6 hour time point (Figure 2f). The order of focus assembly we have observed in IMR90 cells is therefore γ -H2AX first, then Brca1, followed by MRN.

We also examined the appearance of Rad51 foci after ionizing radiation and found that these foci are present in only a subset of IMR90 cells and this subset largely overlapped the subset that exhibited Brca1 foci. When we stained unirradiated cells with Rad51 antibody, we found that very few of the S phase Rad51 foci overlap with γ -H2AX foci (less than 10%; data not shown). After 12 Gy irradiation and 2 hours recovery, Rad51 and Brca1 foci were apparent in 10–15% of the cells but there was no significant overlap between Rad51 foci and γ -H2AX foci at this time (Figure 2g). By 6 hours, however, Rad51 foci were present in 20–25% of the cells and there was a very clear coincidence of Rad51 with γ -H2AX spots (Figure 2h). When we looked at the association of Rad51 with Brca1 at different time points we found that their colocalization increased gradually over the course of the experiment with at least 55% of the total number of Rad51 foci colocalizing with Brca1 foci after 6 hours of recovery (Figure 2i and quantification in Figure 3b). In general, we observed that Rad50 and Rad51 were not found in the same individual cell nuclei, similar to previous reports [1,23]. Thus, the time course of Rad51– γ -H2AX colocalization we observed was similar to that of Rad50– γ -H2AX, although in different subsets of cells, and occurred later during recovery than Brca1 colocalization with γ -H2AX.

To extend the results we obtained with the IMR90 cell line, we also tested SVG p12 cells, an SV40-transformed

Figure 3



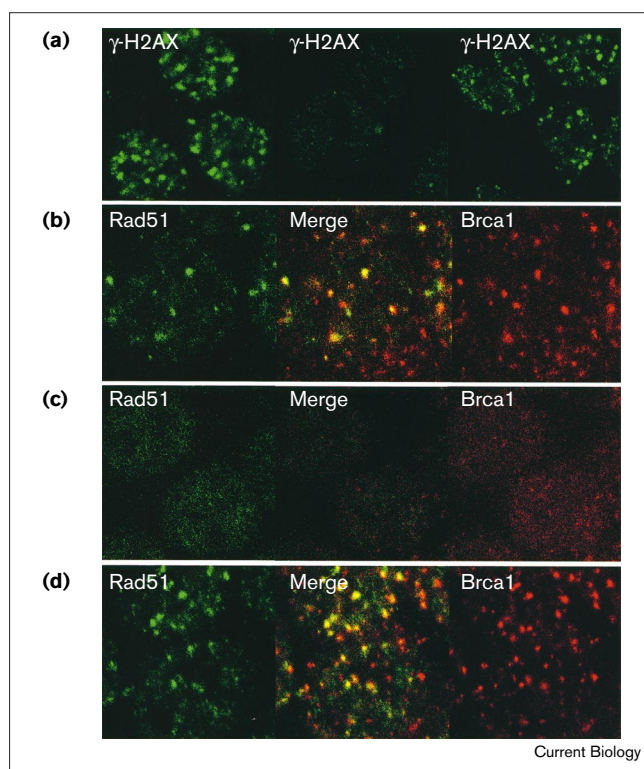
Quantification of radiation-induced foci. (a) IMR90 cells, either unirradiated or irradiated with 12 Gy, were stained with γ -H2AX and Rad50 antibodies, as in Figure 2a–c. At least 30 images were collected from each time point and the number of overlapping foci was determined using NIH Image. Foci were counted in this way for each time point: unirradiated (0) or irradiated (0.5, 2, 4, 6 and 8 h recovery). The sets of data from each time point exhibited Poisson distributions, and the average value for each data set is plotted on the graph. The Y axis represents the number of foci per average cell nucleus area. The number of γ -H2AX–Rad50 overlapping foci (filled diamonds) is represented in comparison with the total number of γ -H2AX foci (open squares). (b) An analysis of γ -H2AX–Brca1 overlapping foci (open squares) is shown in comparison to Brca1–Rad51 overlapping foci (closed squares) at four different time points: 0 (unirradiated cells), 45 min, 2 h, and 6 h, using methods described in (a).

human fibroblast line. In these cells, the order of focus formation was the same as that observed in the IMR90 cells, namely γ -H2AX first, followed by Brca1– γ -H2AX, followed by Rad50– γ -H2AX or Rad51– γ -H2AX colocalization in different subsets of cells (data not shown). In the transformed cells, however, the Brca1 association with γ -H2AX appeared as early as 45 minutes after irradiation, suggesting that the absolute amount of time required for recruitment of factors to the sites of DNA damage can vary dramatically among cell lines. In addition, the proportion of cells containing Rad51 foci was much higher in SVG p12 than in IMR90, both before irradiation (30% versus 10%) and after irradiation (60% versus 20%). Overall, our examination of γ -H2AX colocalization with these repair factors in multiple cell lines suggests that all damage-induced nuclear foci, both Rad50 and Rad51 types, originate as γ -H2AX foci.

Wortmannin inhibits radiation-induced focus formation

Although the kinase responsible for phosphorylation of H2AX molecules in mammalian cells after irradiation has not been described, the phosphorylation site in the H2AX carboxy-terminal tail does match the ‘SQ’ consensus phosphorylation sequence for the DNA-dependent protein kinase (DNA-PK), which is known to be involved in the cellular response to ionizing radiation [27,28]. DNA-PK is a member of a subfamily of protein kinases, including ATM (Ataxia–Telangiectasia mutated) and ATR (Rad3-related) proteins, which show homology to the PI-3 group

Figure 4



Wortmannin inhibits focus formation. **(a)** MCF7 cells were irradiated with 12 Gy ionizing radiation and were allowed to recover for 1 h at 37° before fixation with antibodies directed against γ -H2AX. Cells received either no drug (left panel), were preincubated with 200 μ M wortmannin (middle panel), or were incubated with the wortmannin starting 5 min after irradiation (right panel). **(b–d)** MCF7 cells were treated as in **(a)** and then stained with antibodies directed against Rad51 (green) and Brca1 (red). Cells either **(b)** received no drug, **(c)** were preincubated with wortmannin, or **(d)** were exposed to wortmannin starting 5 min after irradiation. The kinetics of focus formation in MCF7 cells are considerably faster than in IMR90 cells; the 1 h time point shown here was found to yield the most foci after radiation treatment in MCF7 cultures.

of lipid kinases [29–33]. Like the lipid kinases, this subfamily of protein kinases can be inhibited by the fungal metabolite wortmannin [34–39]. To investigate the role of these kinases in focus formation, we incubated cells with the drug before or after exposure to ionizing radiation, and stained with antibodies specific for γ -H2AX, Brca1, and Rad51, as shown in Figure 4.

Compared with untreated MCF7 cells (Figure 4a, left), cells incubated with wortmannin for 30 minutes prior to 12 Gy irradiation had substantially fewer and much less bright γ -H2AX foci (Figure 4a, middle). Staining of these cells with antibodies specific for Brca1 and Rad51 showed that the wortmannin preincubation completely eliminated focus formation by these proteins as well (Figure 4c; compare with the irradiated cells incubated without the drug,

Figure 4b). In contrast, if wortmannin was added within 5 minutes after radiation (a time point after the appearance of γ -H2AX foci but before the appearance of Brca1–Rad51 foci), all the foci appeared normally (Figure 4a, right, and Figure 4d). Therefore, the wortmannin-sensitive step in focus formation occurs very early in the response to irradiation and is likely to be the phosphorylation of γ -H2AX itself. Elimination of γ -H2AX focus formation by wortmannin prevented focus formation by the other factors, suggesting that phosphorylation of H2AX is a necessary step in this pathway. We have not found any conditions of wortmannin treatment that permitted Brca1–Rad51 focus formation in the absence of γ -H2AX foci.

γ -H2AX focus formation in repair-deficient cells

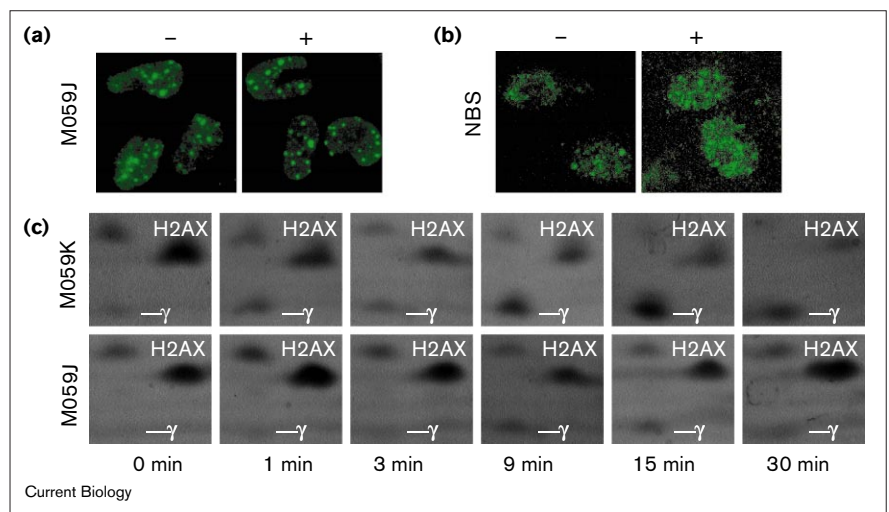
Given the dramatic effect of wortmannin treatment on focus formation in MCF7 cells, we then examined the response to irradiation in M059J cells, which are known to be completely deficient in DNA-PK [40] and have extremely low levels of ATM protein [41–43]. Surprisingly, we found that M059J cells exhibited a high level of γ -H2AX foci even during normal growth conditions (Figure 5a, ‘–’). Exposure of these cells to ionizing irradiation did not increase the number of foci per cell (Figure 5a, ‘+’).

Because visual focus formation may not reflect subtle changes in the amount of γ -H2AX formed *in vivo*, we exposed M059J cells to a high level of radiation (200 Gy) and compared the levels of phosphorylated versus unphosphorylated H2AX on Coomassie-stained two-dimensional protein gels compared to M059K cells, a DNA-PK positive control (Figure 5c). (The high X-ray dose is necessary here in order to see the change in H2AX phosphorylation state biochemically; the constitutive level of γ -H2AX foci in unirradiated M059J cells is far below the minimum amount at which phosphorylated protein would be visible in gels). In the DNA-PK-positive cells, the phosphorylated form of the histone increased dramatically over the time course of recovery, reaching a maximum of approximately 70% of the total H2AX in the cell. In the M059J cells, there was a small increase in the amount of γ -H2AX, but it was several-fold reduced compared to the normal cell line (Figure 5c and [24]). From these results we conclude that the absence of DNA-PK and ATM substantially reduces the γ -H2AX response, but does not eliminate it. A kinase other than DNA-PK must therefore also be able to phosphorylate the histone and does so in M059J cells even in the absence of external sources of ionizing radiation.

We also examined an NBS cell line, which contains a mutated version of the Nijmegen breakage syndrome (NBS) gene, exhibits high levels of chromosomal aberrations after exposure to ionizing radiation [44], and does not exhibit MRN foci (data not shown). Like the M059J cell line, we observed high levels of γ -H2AX foci in unirradiated cultures, as shown in Figure 5b, ‘–’. At least 50–70%

Figure 5

Repair-deficient cell lines exhibit abnormal γ -H2AX focus formation. **(a)** M059J cells, either untreated (–) or irradiated with 0.6 Gy (+), were fixed, permeabilized, and stained with antibodies directed against γ -H2AX. The irradiated cells recovered for 4.5 h at 37° before fixation. **(b)** NBS fibroblasts, either untreated (–) or irradiated with 2 Gy (+), were fixed and permeabilized as described in Figure 1 and stained with antibodies directed against γ -H2AX. The irradiated cells recovered for 4 h at 37° before fixation. **(c)** M059J (DNA-PK-deficient) and M059K (DNA-PK-positive) cells were irradiated with 200 Gy and incubated at 37° for varying times as indicated before histone extraction, 2-D gel analysis, and Coomassie staining. The locations of the unphosphorylated (H2AX) and phosphorylated (γ) forms of the histone are indicated in each panel.



of unirradiated cells contained γ -H2AX foci, compared to 5–10% of normal fibroblasts. NBS cells exhibit high levels of chromosomal instability [44], so the presence of many γ -H2AX foci may be a visual indication of an increased incidence of double-strand breaks in these cells. Unlike the M059J cells, however, the NBS cells exhibited a 5- to 10-fold increase in the number of γ -H2AX foci after exposure to 2 Gy irradiation (Figure 5b, '+'). In addition, the Brca1 and Rad51 colocalization with γ -H2AX appeared to occur normally in these cells (data not shown), thus formation of MRN foci is not necessary for these responses.

Discussion

In this work we have investigated the relationship between the phosphorylation of histone H2AX and the sequestration of repair factors following DNA damage. The use of a laser scissors apparatus to introduce double-strand breaks at very precise locations in cell nuclei enabled us to observe the phosphorylated histone molecule as well as the MRN complex and Brca1 directly at the sites of the breaks. The colocalization of foci after exposure to ionizing radiation also indicated that Brca1 and Rad50 (or Rad51) foci form sequentially at sites of H2AX phosphorylation. Blockage of γ -H2AX foci with the kinase inhibitor wortmannin suppressed the later focus formation by the repair-related factors, suggesting a causal link between these responses. A cell line deficient in DNA-PK and ATM showed very little increase in H2AX focus formation after DNA damage, although the cells exhibited constitutive γ -H2AX foci in unirradiated cultures. The appearance of foci of H2AX before the repair factors, and the dependence of all these foci on the prior phosphorylation of H2AX, suggests that H2AX phosphorylation and focus formation is a necessary first step in the organization of repair factor foci. These results also suggest a role for

DNA-PK and ATM in focus formation by γ -H2AX and the other repair factors in response to DNA damage, and a potential role for another PI-3-type protein kinase that can function constitutively in their absence.

An ordered recruitment of factors to sites of DNA damage

Examination of focus formation following irradiation in several different cell lines led us to the conclusion that, although Rad50 and Rad51 appear to form foci in different subsets of cells, each repair factor colocalized over time with sites of H2AX phosphorylation. This finding links the two types of repair complexes to a common initiating signal and suggests that in both cases, the repair molecules are recruited to specific domains of chromatin containing damaged DNA.

Interestingly, when we looked at Brca1– γ -H2AX colocalization in comparison to Rad50 and Rad51, we found that Brca1 is recruited to sites of γ -H2AX phosphorylation several hours before the other factors. This was quite surprising because Brca1 has no reported DNA-binding properties and we had expected it to be recruited to sites of double-strand breaks by DNA-binding factors like Rad51 and MRN. The order of assembly instead appears to be the opposite, with Brca1 'upstream' of both Rad50 and Rad51. The same order was observed in the transformed SVG p12 cell line, although the absolute amount of time required was less (45 minutes compared with 2 hours).

Like Zhong *et al.* [23], we observed colocalization of Brca1 with the MRN complex; however, we did not see this in all cells containing MRN foci. In all the cell lines we examined, a large proportion of the population of cells with MRN foci did not exhibit Brca1 foci. Since Brca1 and Rad51 form foci in S phase, it will be very interesting to

determine how cell cycle stage affects partitioning of a cell population between Rad50 and Rad51 focus-containing cells and how this affects Brca1 localization.

Why foci?

With all the repair factors we studied, the intensity of individual foci increased gradually over time, as did the extent of colocalization within individual cells. By the time a factor is visible as a distinct focus, hundreds or thousands of molecules must be present at that site. Why so many repair molecules would be necessary at the site of one or a few double-strand breaks is not known. The visible accumulation of factors at sites of DNA damage may be an indication of a checkpoint mechanism used by the cell, instead of a visualization of DNA repair which theoretically would require only one set of repair enzymes to rejoin the DNA or perform homologous recombination. Consistent with this view, cell lines with known deficiencies in MRN focus formation (AT [1], NBS [45], and AT-like disorder [46]) do not exhibit significantly lower levels of DNA repair, but do show extreme problems with checkpoint functions.

Another hypothesis for the function of foci in DNA repair, not necessarily contradictory to those already mentioned, is the possibility that the foci occur at sites where the repair machinery has difficulty repairing the breaks that are present. It is known that radiation-induced double-strand breaks are not evenly distributed throughout the nucleus but occur in clusters, as a result of multiple ionization events along a radiation track [47,48]. These multiply-damaged sites are likely to be the substrates of the 'slow' component of DNA repair, using current models of biphasic double-strand break kinetics [49]. Although it seems clear that the kinetics of focus formation in normal human fibroblasts are not consistent with the kinetics of 'fast' repair ($t_{1/2}$ estimated to be 30 minutes or less), it would be consistent with the kinetics of the 'slow' component ($t_{1/2}$ estimated between 1 and 4 hours) [50–53]. In light of this model, accumulation of repair factors as foci would be a visible indication of the large concentration of repair activity at multiply-damaged sites. Interestingly, a defective 'slow' component of repair has been implicated in *xrs-5* rodent cells, which lack the DNA end-binding protein Ku80 and show an inability to repair multiply-damaged chromatin loops [54].

Phosphorylation of histone H2AX

Members of the PI-3 kinase-like family, including DNA-PK, ATM, and ATR, have been implicated as important components of the biological response to DNA damage [27,30,55], thus making them excellent candidates for the kinases responsible for phosphorylating H2AX. The fungal metabolite wortmannin is known to be a potent inhibitor of PI-3 type lipid kinases and is also effective against the protein kinases in this superfamily [36,38,39].

In our experiments we found that preincubation with wortmannin inhibited focus formation by γ -H2AX, as well as focus formation by Brca1 and Rad51, suggesting that PI-3-related kinases may indeed be involved in this response.

Does the kinase inhibitor block focus formation through its effect on H2AX phosphorylation, or by another route? We approached this question by adding wortmannin either before or after irradiation, reasoning that H2AX phosphorylation appears to be the earliest detectable event after DNA damage. It was remarkable that wortmannin added just after irradiation completely lost its inhibitory effect on γ -H2AX foci and on the later focus formation of Brca1 or Rad51, even though the cells were exposed to wortmannin long before the Brca1 and Rad51 foci usually appeared. This observation suggests that H2AX phosphorylation may be an initiating event in the process of focus formation, and that the absence of Brca1–Rad51 foci after preincubation in wortmannin is a direct result of the absence of H2AX phosphorylation.

In our experiments, the concentration of wortmannin required for inhibition of focus formation was quite high (200 μ M). One possible explanation for the resistance of the H2AX phosphorylation to the drug is that ATR is 10- to 100-fold less sensitive to wortmannin compared to DNA-PK and ATM [39]. *In vivo* experiments have shown that half-maximal inhibition of ATR is achieved only with concentrations higher than 100 μ M.

Because wortmannin affects numerous kinases of the PI-3 family, we also examined focus formation in cells lacking specific PI-3 kinases. The only human cell line known to be deficient in DNA-PK is the M059J tumor cell line, which also has very low levels of ATM [41–43]. Our analysis of the M059J cell line indicates that DNA-PK and ATM are likely playing a role in this response because the cells show a dramatically reduced ability to phosphorylate H2AX in response to DNA damage. There must be some redundancy in this function, however, because the M059J cells do exhibit a small increase in H2AX phosphorylation, and because the cells exhibit a large number of γ -H2AX foci even without any external source of DNA damage. As phosphorylation of H2AX is specific to double-strand breaks [24], this very likely indicates a high level of breaks present in the cells all the time. It is not yet clear whether these foci represent many breaks being made with a high turnover of repair, or whether there are relatively few breaks that persist in the cells for a longer time without being repaired. The ATR and ATM homologs Mec1 and Tel1 are already known to be partially redundant in yeast, in which they function in both DNA damage checkpoints as well as in telomere maintenance [56–58].

Like the M059J cells, NBS cells also show γ -H2AX foci in the absence of irradiation but the number of foci clearly

increases after exposure to ionizing radiation. Thus, the MRN complex does not function in the formation of γ -H2AX foci. In addition, focus formation by Brca1 and Rad51 is unchanged in these cells, consistent with MRN being downstream from Brca1 and functionally separate from Rad51.

Chromatin structure and DNA repair

The colocalization of repair factors with modified histone molecules could be important not only in signalling the location of double-strand breaks but also in changing the local chromatin structure around the break. The carboxy-terminal tails of H2A histone molecules have been shown to contact the 'linker' region of nucleosomal DNA and histone H1 [59,60], and can affect the condensation of the chromatin fiber [61]. Thus, modification of the H2AX tail by phosphorylation may change the overall structure of the chromosomal domain containing a break, as well as the accessibility of the fiber to other factors. Consideration of chromatin structure will have to become an essential part of the study of double-strand break repair as we try to understand how the first signal of a break is transmitted to the repair factors and cell cycle control machinery.

Conclusions

Comparison of focus formation by γ -H2AX, the Mre11–Rad50–Nbs1 complex, Brca1, and Rad51 suggests that γ -H2AX localization precedes and initiates focus formation by the repair-related factors. The data also support a role for DNA-PK, ATM, and the PI-3 kinase-like family of protein kinases in this response.

Materials and methods

Laser scissors and ionizing radiation

MCF7 cells were grown in RPMI medium (Gibco BRL) containing 0.4 μ M BrdU and 2.4 μ M thymidine for 3 days and were subcultured onto coverslips in the same medium. When the cells grew to 50–70% confluence, the cover slips were incubated with 10 μ g/ml Hoechst dye 33258 in phosphate-buffered saline (PBS) for 10 min at 37°. The cover slips were mounted onto glass slides with a layer of PBS between the cover slips and the slides, using 0.5 mm silicon gaskets (Molecular Probes). The slides were kept on ice until mounting on the stage of a microscope fitted with a LaserScissors module 390/20 (Cell Robotics). The laser was focused through a 100 \times objective and operated at various power outputs ranging from 1–30%, using a pulse rate set at 10 pulses/s, and movement of the stage was controlled using a joystick. After irradiation, the coverslips were transferred to culture dishes and incubated at 37° for varying amounts of time as described in Figure 1. At the lowest laser setting (1% of full power), the beam generates 1000 kJ/m², which translates into a conservative estimate of > 80 Gy using standard absorption coefficients.

IMR90, MCF7, SVG p12, M059J, M059K and NBS cells were irradiated with a ¹³⁷Cs source in a Mark I irradiator (J.L. Shepherd and Assoc.) and allowed to recover at 37° for various amounts of time as indicated in Figures 2,4,5.

Immunostaining

Cells were fixed either with methanol or with 3% paraformaldehyde + 2% sucrose for 10 min. Permeabilization was performed with acetone after methanol fixation [1] or with a 0.5% Triton wash after formaldehyde

[4]. The Triton wash did not make a significant difference for γ -H2AX or Rad50 staining, but greatly improved the intensity of the Brca1 and Rad51 staining. The polyclonal antibody directed against γ -H2AX was prepared as described [25]. Other polyclonal antibodies were directed against Rad51 (Ab-1, Oncogene) and Nbs1 (Novus Biologicals). Monoclonal antibodies were specific for Rad50 (13-B3, Genetex), Brca1 (Ab-1, Oncogene), and Rad51 (gift of Wen-Hwa Lee). All primary antibodies were used at dilutions of 1:200 to 1:800. The secondary antibodies included anti-rabbit FITC and anti-mouse Alexa 546 (Molecular Probes) and were used at dilutions of 1:200. Immunofluorescence images were captured using a laser scanning confocal microscope (Nikon PCM2000). All red channel images were taken with the He-Ne laser only (argon laser blocked).

Quantification of foci

IMR90 cells, either unirradiated or irradiated with 12 Gy, were stained with combinations of antibodies directed against γ -H2AX and Rad50 (Figure 3a), γ -H2AX and Brca1 (Figure 3b), or Brca1 and Rad51 (Figure 3b). At least 30 images were randomly collected from each time point shown, with the 0 time point representing the unirradiated population. The foci in each channel (red and green) for each image were counted separately using the software program NIH Image. The result files from each measurement were superimposed on each other to determine the number of overlapping foci. The area of the nucleus in each image was also determined and used to adjust the count with respect to the average nuclei area, because nucleus size varied considerably within the cell population. The set of data from each time point exhibited a Poisson distribution, and the average values from each data set are represented on the graphs shown in Figure 3.

NBS cells

Primary fibroblasts from an NBS patient of eastern European origin [62] were retrovirally transformed with the HPV E6 and E7 genes. 10⁹ cells were maintained for several months until crisis occurred; a single transformant (growing into a colony) was isolated.

Three-dimensional gel analysis of H2AX

M059J and M059K cell cultures in ice cold media were exposed to 200 Gy. After irradiation the cold media was replaced with media at 37°C and the cultures placed in an incubator for the times indicated. Histone extraction and two-dimensional gel analysis were performed as previously described [24].

Acknowledgements

We thank Wen-Hwa Lee for the anti-Rad51 antibody and our colleagues in the Laboratory of Molecular Biology for helpful comments. T.T.P. was supported by a Helen Hay Whitney Postdoctoral Fellowship.

References

1. Maser RS, Monsen KJ, Nelms BE, Petrini JH: **hMre11 and hRad50 nuclear foci are induced during the normal cellular response to DNA double-strand breaks.** *Mol Cell Biol* 1997, **17**:6087-6096.
2. Haaf T, Golub EI, Reddy G, Radding CM, Ward DC: **Nuclear foci of mammalian Rad51 recombination protein in somatic cells after DNA damage and its localization in synaptonemal complexes.** *Proc Natl Acad Sci USA* 1995, **92**:2298-2302.
3. Liu Y, Li M, Lee EY, Maizels N: **Localization and dynamic relocation of mammalian rad52 during the cell cycle and in response to DNA damage.** *Curr Biol* 1999, **9**:975-978.
4. Scully R, Chen J, Ochs RL, Keegan K, Hoekstra M, Feunteun J, *et al.*: **Dynamic changes of BRCA1 subnuclear location and phosphorylation state are initiated by DNA damage.** *Cell* 1997, **90**:425-435.
5. Raderschall E, Golub EI, Haaf T: **Nuclear foci of mammalian recombination proteins are located at single-stranded DNA regions formed after DNA damage.** *Proc Natl Acad Sci USA* 1999, **96**:1921-1926.
6. Reimer CL, Borrás AM, Kurdistani SK, Garreau JR, Chung M, Aaronson SA, *et al.*: **Altered regulation of cyclin G in human breast cancer and its specific localization at replication foci in response to DNA damage in p53+/+ cells.** *J Biol Chem* 1999, **274**:11022-11029.

7. Nelms BE, Maser RS, MacKay JF, Lagally MG, Petrini JH: *In situ* visualization of DNA double-strand break repair in human fibroblasts. *Science* 1998, **280**:590-592.
8. Game JC, Mortimer RK: A genetic study of x-ray sensitive mutants in yeast. *Mutat Res* 1974, **24**:281-292.
9. Ivanov EL, Korolev VG, Fabre F: XRS2, a DNA repair gene of *Saccharomyces cerevisiae*, is needed for meiotic recombination. *Genetics* 1992, **132**:651-664.
10. Johzuka K, Ogawa H: Interaction of Mre11 and Rad50: two proteins required for DNA repair and meiosis-specific double-strand break formation in *Saccharomyces cerevisiae*. *Genetics* 1995, **139**:1521-1532.
11. Boulton SJ, Jackson SP: Components of the Ku-dependent non-homologous end-joining pathway are involved in telomeric length maintenance and telomeric silencing. *EMBO J* 1998, **17**:1819-1828.
12. Lewis LK, Westmoreland JW, Resnick MA: Repair of endonuclease-induced double-strand breaks in *Saccharomyces cerevisiae*: essential role for genes associated with nonhomologous end-joining. *Genetics* 1999, **152**:1513-1529.
13. Game JC: DNA double-strand breaks and the RAD50-RAD57 genes in *Saccharomyces*. *Sem Cancer Biol* 1993, **4**:73-83.
14. Kironmai KM, Muniyappa K: Alteration of telomeric sequences and senescence caused by mutations in RAD50 of *Saccharomyces cerevisiae*. *Genes Cells* 1997, **2**:443-455.
15. Nugent CI, Bosco G, Ross LO, Evans SK, Salinger AP, Moore JK, et al.: Telomere maintenance is dependent on activities required for end repair of double-strand breaks. *Curr Biol* 1998, **8**:657-660.
16. Le S, Moore JK, Haber JE, Greider CW: RAD50 and RAD51 define two pathways that collaborate to maintain telomeres in the absence of telomerase. *Genetics* 1999, **152**:143-152.
17. Ivanov EL, Sugawara N, White CI, Fabre F, Haber JE: Mutations in XRS2 and RAD50 delay but do not prevent mating-type switching in *Saccharomyces cerevisiae*. *Mol Cell Biol* 1994, **14**:3414-3425.
18. Bressan DA, Baxter BK, Petrini JH: The Mre11-Rad50-Xrs2 protein complex facilitates homologous recombination-based double-strand break repair in *Saccharomyces cerevisiae*. *Mol Cell Biol* 1999, **19**:7681-7687.
19. Paull TT, Gellert M: The 3' to 5' exonuclease activity of Mre11 facilitates repair of DNA double-strand breaks. *Mol Cell Biol* 1998, **18**:969-979.
20. Paull TT, Gellert M: Nbs1 potentiates ATP-driven DNA unwinding and endonuclease cleavage by the Mre11/Rad50 complex. *Genes Dev* 1999, **13**:1276-1288.
21. Trujillo KM, Yuan SS, Lee EY, Sung P: Nuclease activities in a complex of human recombination and DNA repair factors Rad50, Mre11, and p95. *J Biol Chem* 1998, **273**:21447-21450.
22. Tashiro S, Kotomura N, Shinohara A, Tanaka K, Ueda K, Kamada N: S phase specific formation of the human Rad51 protein nuclear foci in lymphocytes. *Oncogene* 1996, **12**:2165-2170.
23. Zhong Q, Chen CF, Li S, Chen Y, Wang CC, Xiao J, et al.: Association of BRCA1 with the hRad50-hMre11-p95 complex and the DNA damage response. *Science* 1999, **285**:747-750.
24. Rogakou EP, Pilch DR, Orr AH, Ivanova VS, Bonner WM: DNA double-stranded breaks induce histone H2AX phosphorylation on serine 139. *J Biol Chem* 1998, **273**:5858-5868.
25. Rogakou EP, Boon C, Redon C, Bonner WM: Megabase chromatin domains involved in DNA double-strand breaks *in vivo*. *J Cell Biol* 1999, **146**:905-916.
26. Limoli CL, Ward JF: A new method for introducing double-strand breaks into cellular DNA. *Radiat Res* 1993, **134**:160-169.
27. Smith GC, Jackson SP: The DNA-dependent protein kinase. *Genes Dev* 1999, **13**:916-934.
28. Bannister AJ, Gottlieb TM, Kouzarides T, Jackson SP: c-Jun is phosphorylated by the DNA-dependent protein kinase *in vitro*; definition of the minimal kinase recognition motif. *Nucleic Acids Res* 1993, **21**:1289-1295.
29. Savitsky K, Bar-Shira A, Gilad S, Rotman G, Ziv Y, Vanagaite L, et al.: A single ataxia telangiectasia gene with a product similar to PI-3 kinase. *Science* 1995, **268**:1749-1753.
30. Zakian VA: ATM-related genes: what do they tell us about functions of the human gene? *Cell* 1995, **82**:685-687.
31. Keith CT, Schreiber SL: PIK-related kinases: DNA repair, recombination, and cell cycle checkpoints. *Science* 1995, **270**:50-51.
32. Hunter T: When is a lipid kinase not a lipid kinase? When it is a protein kinase. *Cell* 1995, **83**:1-4.
33. Hartley KO, Gell D, Smith GC, Zhang H, Divecha N, Connelly MA, et al.: DNA-dependent protein kinase catalytic subunit: a relative of phosphatidylinositol 3-kinase and the ataxia telangiectasia gene product. *Cell* 1995, **82**:849-856.
34. Boulton S, Kyle S, Yalcintepe L, Durkacz BW: Wortmannin is a potent inhibitor of DNA double strand break but not single strand break repair in Chinese hamster ovary cells. *Carcinogenesis* 1996, **17**:2285-2290.
35. Hosoi Y, Miyachi H, Matsumoto Y, Ikehata H, Komura J, Ishii K, et al.: A phosphatidylinositol 3-kinase inhibitor wortmannin induces radioresistant DNA synthesis and sensitizes cells to bleomycin and ionizing radiation. *Int J Cancer* 1998, **78**:642-647.
36. Okayasu R, Suetomi K, Ullrich RL: Wortmannin inhibits repair of DNA double-strand breaks in irradiated normal human cells. *Radiat Res* 1998, **149**:440-445.
37. Price BD, Youmell MB: The phosphatidylinositol 3-kinase inhibitor wortmannin sensitizes murine fibroblasts and human tumor cells to radiation and blocks induction of p53 following DNA damage. *Cancer Res* 1996, **56**:246-250.
38. Rosenzweig KE, Youmell MB, Palayoor ST, Price BD: Radiosensitization of human tumor cells by the phosphatidylinositol 3-kinase inhibitors wortmannin and LY294002 correlates with inhibition of DNA-dependent protein kinase and prolonged G2-M delay. *Clin Cancer Res* 1997, **3**:1149-1156.
39. Sarkaria JN, Tibbetts RS, Busby EC, Kennedy AP, Hill DE, Abraham RT: Inhibition of phosphoinositide 3-kinase related kinases by the radiosensitizing agent wortmannin. *Cancer Res* 1998, **58**:4375-4382.
40. Lees-Miller SP, Godbout R, Chan DW, Weinfeld M, Day RS 3rd, Barron GM, et al.: Absence of p350 subunit of DNA-activated protein kinase from a radiosensitive human cell line. *Science* 1995, **267**:1183-1185.
41. Hoppe BS, Jensen RB, Kirchgessner CU: Complementation of the radiosensitive M059J cell line. *Radiat Res* 2000, **153**:125-130.
42. Gately DP, Hittle JC, Chan GK, Yen TJ: Characterization of ATM expression, localization, and associated DNA-dependent protein kinase activity. *Mol Biol Cell* 1998, **9**:2361-2374.
43. Chan DW, Gately DP, Urban S, Galloway AM, Lees-Miller SP, Yen T, et al.: Lack of correlation between ATM protein expression and tumour cell radiosensitivity. *Int J Radiat Biol* 1998, **74**:217-224.
44. Shiloh Y: Ataxia-telangiectasia and the Nijmegen breakage syndrome: related disorders but genes apart. *Annu Rev Genet* 1997, **31**:635-662.
45. Carney JP, Maser RS, Olivares H, Davis EM, Le Beau M, Yates JR, 3rd, et al.: The hMre11/hRad50 protein complex and Nijmegen breakage syndrome: linkage of double-strand break repair to the cellular DNA damage response. *Cell* 1998, **93**:477-486.
46. Stewart GS, Maser RS, Stankovic T, Bressan DA, Kaplan ML, Jaspers NG, et al.: The DNA double-strand break repair gene hMre11 is mutated in individuals with an Ataxia-Telangiectasia-like disorder. *Cell* 1999, **99**:577-587.
47. Rydberg B: Clusters of DNA damage induced by ionizing radiation: formation of short DNA fragments. II. Experimental detection. *Radiat Res* 1996, **145**:200-209.
48. Goodhead DT: Initial events in the cellular effects of ionizing radiations: clustered damage in DNA. *Int J Radiat Biol* 1994, **65**:7-17.
49. Iliakis G: The role of DNA double strand breaks in ionizing radiation-induced killing of eukaryotic cells. *Bioessays* 1991, **13**:641-648.
50. Wheeler KT, Nelson GB: Saturation of a DNA repair process in dividing and nondividing mammalian cells. *Radiat Res* 1987, **109**:109-117.
51. van Rongen E, Thames HD Jr, Travis EL: Recovery from radiation damage in mouse lung: interpretation in terms of two rates of repair. *Radiat Res* 1993, **133**:225-233.
52. Metzger L, Iliakis G: Kinetics of DNA double-strand break repair throughout the cell cycle as assayed by pulsed field gel electrophoresis in CHO cells. *Int J Radiat Biol* 1991, **59**:1325-1339.
53. Dikomey E, Lorenzen J: Saturated and unsaturated repair of DNA strand breaks in CHO cells after X-irradiation with doses ranging from 3-90 Gy. *Int J Radiat Biol* 1993, **64**:659-667.
54. Johnston PJ, Bryant PE: A component of DNA double-strand break repair is dependent on the spatial orientation of the lesions within the higher-order structures of chromatin. *Int J Radiat Biol* 1994, **66**:531-536.

55. Hoekstra MF: **Responses to DNA damage and regulation of cell cycle checkpoints by the ATM protein kinase family.** *Curr Opin Genet Dev* 1997, **7**:170-175.
56. Sanchez Y, Desany BA, Jones WJ, Liu Q, Wang B, Elledge SJ: **Regulation of RAD53 by the ATM-like kinases MEC1 and TEL1 in yeast cell cycle checkpoint pathways.** *Science* 1996, **271**:357-360.
57. Ritchie KB, Mallory JC, Petes TD: **Interactions of TLC1 (which encodes the RNA subunit of telomerase), TEL1, and MEC1 in regulating telomere length in the yeast *Saccharomyces cerevisiae*.** *Mol Cell Biol* 1999, **19**:6065-6075.
58. Morrow DM, Tagle DA, Shiloh Y, Collins FS, Hieter P: **TEL1, an *S. cerevisiae* homolog of the human gene mutated in ataxia telangiectasia, is functionally related to the yeast checkpoint gene MEC1.** *Cell* 1995, **82**:831-840.
59. Lindsey GG, Orgeig S, Thompson P, Davies N, Maeder DL: **Extended C-terminal tail of wheat histone H2A interacts with DNA of the 'linker' region.** *J Mol Biol* 1991, **218**:805-813.
60. Bonner WM, Stedman JD: **Histone 1 is proximal to histone 2A and to A24.** *Proc Natl Acad Sci USA* 1979, **76**:2190-2194.
61. Hacques MF, Muller S, De Murcia G, Van Regenmortel MH, Marion C: **Use of an immobilized enzyme and specific antibodies to analyse the accessibility and role of histone tails in chromatin structure.** *Biochem Biophys Res Commun* 1990, **168**:637-643.
62. Yamazaki V, Wegner RD, Kirchgessner CU: **Characterization of cell cycle checkpoint responses after ionizing radiation in Nijmegen breakage syndrome cells.** *Cancer Res* 1998, **58**:2316-2322.

Because *Current Biology* operates a 'Continuous Publication System' for Research Papers, this paper has been published on the internet before being printed. The paper can be accessed from <http://biomednet.com/cbiology/cub> – for further information, see the explanation on the contents page.